Classification of Human Balance Recovery Strategies Through Kinematic Motor Synergy Analysis

Keli Shen, Ahmed Chemori, Mitsuhiro Hayashibe

Classification of Human Balance Recovery Strategies Through Kinematic Motor Synergy Analysis

Keli Shen[1], Ahmed Chemori[2] and Mitsuhiro Hayashibe[1]

***Abstract*— A key problem in human balance recovery lies in understanding the mechanism of balance behavior with redundant bio-mechanical motors. Motor synergy has been known as an efficient tool to analyze characteristics of motion behavior and reconstruct control command. In this paper, motor synergy analysis for different control strategies is proposed to analyze different balance motion coordination for various levels of pushing force, and understand the coordination of human multiple joints regarding balance recovery. The spatial synergy of specific joint angles for different pushing force levels exerted on the subject's back is computed with the principal component analysis (PCA) to evaluate the adaptive balance motion response patterns and illustrate the improvement of balance robustness through the switch of joint coordination. Therefore, the switch of postural coordination over multiple joints in balance recovery movements was analyzed to better understand the mechanism of balance strategy generation in this study.**

I. INTRODUCTION

The mechanism of human balance recovery has been studied in the literature where various balance control approaches such as static and stepping strategies have been proposed [1], [2]. Understanding balance strategy is crucial for the elderly population rehabilitation training due to a decrease in standing ability (motor impairment) after losing muscle strength.

Many works related to this research topic have been conducted regarding various aspects. Hip-ankle strategy for balance maintenance was simulated with a double inverted pendulum based on numerical model predictive control [3]. An improved balance strategy with arm usage based on nonlinear model predictive control and its effectiveness was studied in [4], [5]. Besides, another multi-link model including ankle, hip, and neck was proposed in [6] to analyze standing postural control and its motor coordination. However, the aforementioned works were more focused on the human balance control strategy. Indeed, the relation between balance strategies and postural coordination is very important for understanding balance control mechanism [7]. Then, the study in [8] indicates the ability of balance control can be improved with strong coordination over multiple joints.

Synergy was defined as an effective tool to explain the co-work of muscles and joint coordination [9]. A reasonable assumption is that the movement control is simplified by the central nervous system (CNS) through a layered and modular structure. At the lowest level of its hierarchy, muscle employment may be controlled by several functional units, thereby reducing the dimensionality of the output space. Higher levels in the hierarchy may employ and combine these output modules flexibly to control various movements. Consequently, organizing muscle synergy is one way through which the task of controlling a number of degrees of freedom (DoF) is simplified by the CNS. Indeed, two types of synergies were introduced in [10] to describe different structures of muscle patterns that can be shared in motions: (*i*) muscle-related spatial synergy, (*ii*) muscle, and time-related spatiotemporal synergy. In our study, since we only focus on joint coordination across the simplified human model, kinematic spatial motor synergy is employed.

Besides, patterns of coordinated multi-joint motion have been studied in various tasks such as reaching, walking, sit to stand and standing. Coordinating multiple joints in [11] for producing a straight hand path saves a definite computational resource through the multi-joint coordination. The motor synergy of walking motion generated with deep learning has been quantified in Chai's work [12], in which it was concluded that a good synergy level contributes for improving energy efficiency. In sit to stand studies, two aspects have been studied. Yang et al. [13] hava distinguished different standing-up strategies based on recruitment of muscle group and Yamasaki et al. [14] studied joint torques organization and their correlation. The standing coordination has been studied in [6] with a multi-link model including neck, hip, and ankle. However, this work ignored the joint rotation of arms and knees which are definitely useful in our daily life for improving balance ability of quiet standing [4], [5] while applying a pushing force on the back of a human. The main contributions of this paper are summarized as follows.

- An eight-joint model for human balance recovery is proposed and four-level of pushing forces are considered to distinguish different balance strategies.
- Kinematic spatial motor synergy is extracted to classify the organization of joints.
- The switch of balance strategies is discussed according to the space of the extracted synergies.

In this paper, we take kinematic spatial motor synergy analysis into account to classify human balance recovery strategies. This helps us obtain a better understanding of balance control mechanisms in quiet standing from a new viewpoint. The rest of the paper is organized as follows. In section II, the methods of the human experiments are

This work was supported in part by GP-mech Program of Tohoku University, Japan.

[1]Department of Robotics, Graduate School of Engineering, Tohoku University, Sendai, Japan. cumtshenkeli8@gmail.com, hayashibe@tohoku.ac.jp

[2]LIRMM, University of Montpellier, CNRS, Montpellier, France. Ahmed.Chemori@lirmm.fr

described. Data processing is shown in section III and spatial motor synergy is demonstrated in section IV. Section V deals with the obtained result analysis and discussion. Finally, conclusions are made in section VI.

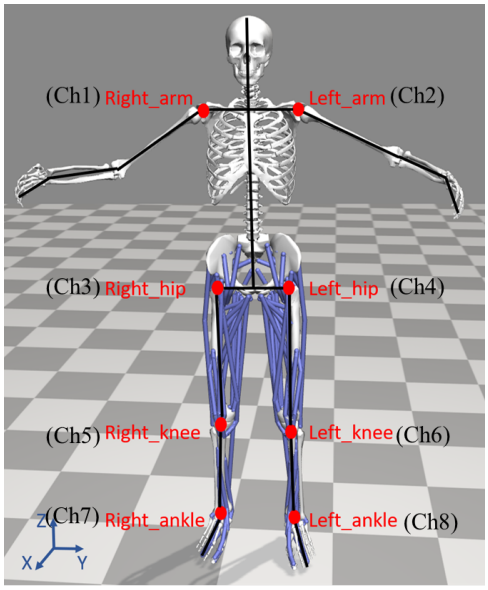

Fig. 1. Structure of the simplified eight-joint model including the joints of right arm, left arm, right hip, left hip, right knee, left knee, right ankle, left ankle. The proposed model setting is consistent with our protocols of human experiments.

II. Methods of Human Experiments

The main purpose of the present study is to explore the relationship between balance recovery strategies and the characteristics of motor synergy for a simplified human body structure as illustrated in Fig. 1. The participants were 6 healthy male subjects (mean age (25 $\pm$ 5) years, mean height (175 $\pm$ 10) cm, mean weight (70 $\pm$ 10) kg) without any known motor or neurological impairment. Following the Declaration of Helsinki, the protocols of human experiments approved by the Tohoku University ethics committee were designed for measuring human postural coordination.

We instructed the subjects to stand upright keeping the two feet on the force-plates (AMTI) [17] to measure the ground reaction force (GrF). First, a static pose with 64 markers was captured for model scaling in Opensim [18]. The marker set of the running model in [19] without head markers was used in our experiments. After completing the static pose, the 22 less important markers for inverse kinematics computation were removed to simplify the process of marker labeling. Then, we asked the subjects to maintain balance through the y-axis rotation of the arm, hip, knee, and ankle joints after a positive x-axis direction disturbing push applied on their back with a stick. This means that human balance motion happens in the sagittal plane. And each time push should be expected with a nearly constant strength. Forty-two marker positions were captured at a frequency of 100 Hz through OptiTrack system [20] to measure body kinematics. Each subject was disturbed with four-level pushing forces on the marked position of the upper back: weak, small, medium, and large for 4 trials separately, and the effect of these forces was measured by inspecting the displacement of the 'C7' marker attached on the neck of each subject. To make each time reaction behavior complete, subjects were pushed the next time after maintaining a balanced position without having the obvious body swaying movements.

III. Data Processing

The conducted experiments include one trial for static pose and 12 trials of balance recovery motion recorded for each subject. Then, we labeled the markers with their names at the beginning of the recording and checked if they were labeled or not frame by frame. After finishing marker labeling, the motion trajectory of each marker was checked, and smoothed by a filter. Then, the recording of marker positions and two force-plates were exported. In fact, the current extracted data form can not be directly used for scaling, inverse kinematics (IK), and inverse dynamics (ID). Therefore, we rearranged data forms of static and dynamic motion, filtered ground reaction forces, and removed force noises.

The converted forms of marker positions and GrF were recruited in Opensim. The data processing in the software Opensim was divided into three steps:

1) **Scaling**: the marker positions of static pose were imported and the height and weight of the subject were necessary for scaling process as well. after scaling, we get a scaling model for the subject. This model can be used for the computation of IK and ID.

2) **Inverse kinematics**: the marker positions of balance recovery motion were imported and the temporal joint angles (around y-axis) of the whole body were computed and extracted.

3) **Inverse dynamics**: the converted forces from the two force-plates were imported and filtered at 6 Hz. Based on the obtained inverse kinematics results and GrF, the temporal joint torques were computed and extracted.

Then, the extracted joint angles and torques of the both-side arm, hip, knee, ankle were normalized between -1 to $+1$ according to the time of the lowest position at z-axis of the marker 'C7'. The time range 1.5 $[s]$ before and 1.5 $[s]$ after the push was employed for the synergy analysis.

IV. Kinematic Spatial Motor Synergy Computation

The definition of Spatial motor synergy has been introduced in [10]. The basic idea is that instantaneous co-variations can be shown by groups of degrees of freedom, indicating adaptive coordination of multiple joints or muscles. This means the hypothesis that the proportion of different control signals should be unchanged over time. This fact be explained by the classical assumption that a set of multiple joints or muscles of the body can be controlled synchronously without specific time-delays by the CNS through reducing the dimension of the DoFs. This can be crucial for saving computational resources of the multiple joint or muscle control, which implies reduced command that

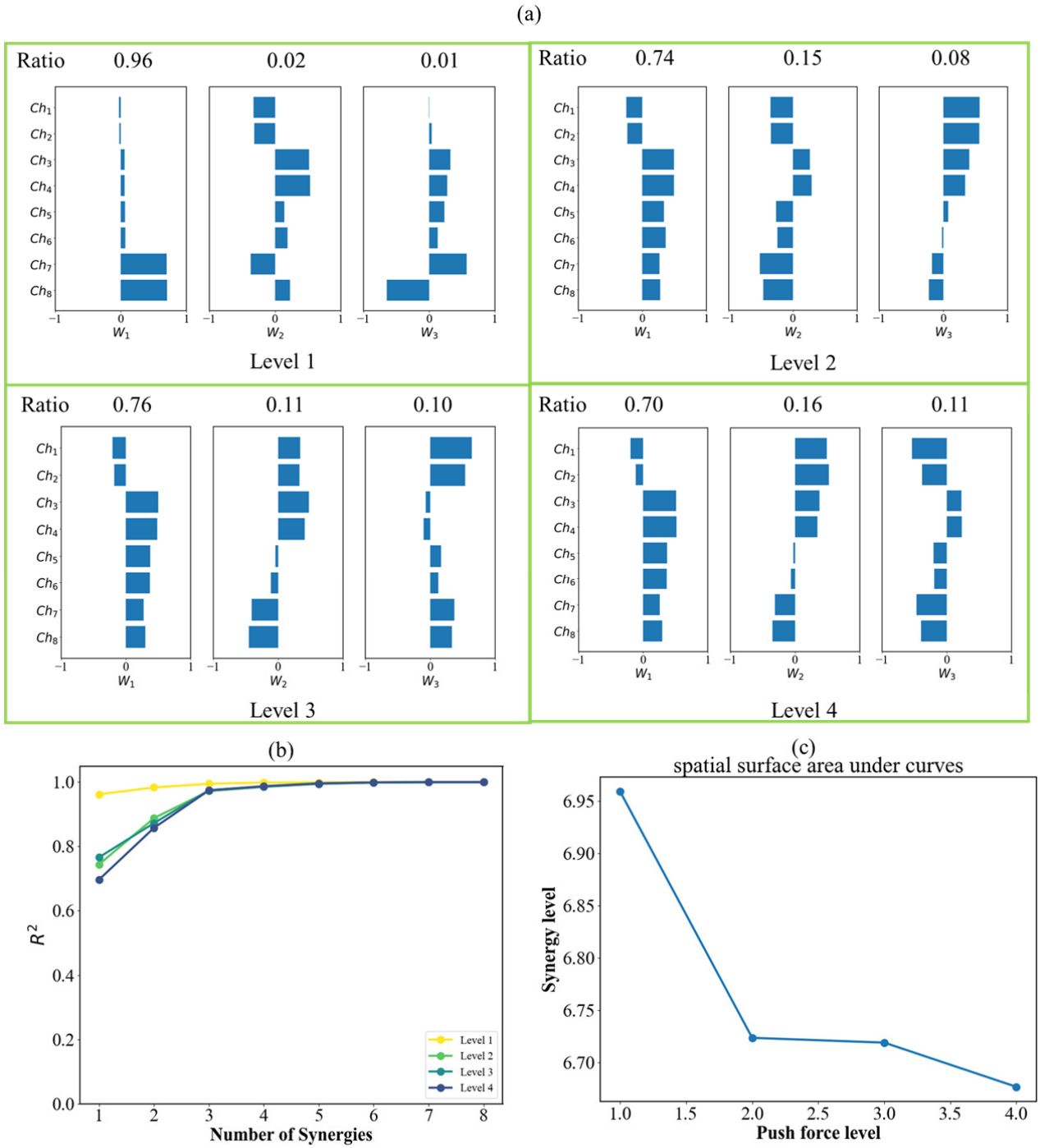

Fig. 2. (*a*) Comparison of the extracted spatial synergies of joint angles for the four-level pushing forces, Ch_1, Ch_2, Ch_3, Ch_4, Ch_5, Ch_6, Ch_7, and Ch_8 represent the angles of the right arm, left arm, right hip, left hip, right knee, left knee, right ankle and left ankle, respectively. (*b*) Reconstruction accuracy for the four-level pushing forces. (*c*) Synergy level computed by spatial surface area under curves of the reconstruction accuracy R^2.

simplifies the complexity of body control. The formulation of the spatial motor synergy is as follows:

$$\mathbf{x}_n^r(t) = \sum_{s=1}^{S} \mathbf{w}_s \cdot c_s^r(t) + \text{ residuals} \tag{1}$$

Where $\mathbf{x}_n^r(t)$ denotes the values of n joint angles rotating around y-axis (For our simplified body model, $1 \leq n \leq 8$) as source signals at time instant t (in our trials, $1 \leq t \leq 300$) in trial number r (in our protocol, $r = 1,\ 2,\ 3,\ 4$). The number of spatial motor synergies is denoted by S. The spatial

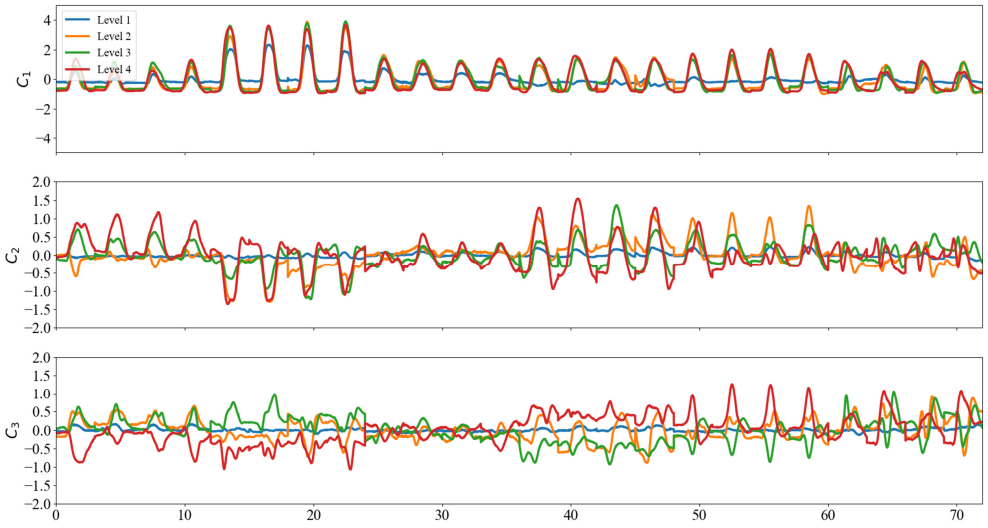

Fig. 3. Corresponding activation weights of the extracted spatial synergies of joint angles for the four-level pushing forces, C_1, C_2, C_3, represent time-related activation where the balance recovery process can be observed.

motor synergy patterns $\mathbf{w}_s$ are extracted as invariant column vectors over trials. The time-dependent mixing weights of the synergies $c_s^r(t)$ and the the residuals vary in each trial.

It is worth to note that the spatial decomposition indicates the contribution of source signals in space. This may help us to easily find which joint-segment might work a lot and how the body joints coordinate according to different pushing force levels in this study. The simplified matrix form of Eq. (1) is derived in Eq. (2), where the term of *residuals* is omitted. X, W, and C represent the matrix of the source signals, the spatial synergies, and the corresponding activation weights, respectively.

$$X = W \cdot C \tag{2}$$

As one of the classical decomposition algorithms, principal component analysis (PCA) [21] is used to solve Eq. (2). The key role of PCA in this study is to minimize the nonlinear least square problem defined as the reconstruction error in Eq. (3) w. r. t W and C with the Frobenius Norm $\|\cdot\|_F$.

$$E^2 = \|X - W \cdot C\|_F^2 \tag{3}$$

The reconstruction accuracy metric R^2 defined in Eq. (4) is used to quantify how well original source signals can be represented by the inner multiplication of the extracted W and the corresponding C term. It is worth to note that R^2 ranges from zero to one. Besides, $R^2 = 1$ indicates the perfect reconstruction of the source signals.

$$R^2 = 1 - \frac{\|X - W \cdot C\|_F^2}{\|X - \bar{X}\|_F^2} \tag{4}$$

In this study, the approach to evaluating joint angles are more synergetic through observing the corresponding joint angles can be reconstructed with fewer spatial synergy and the higher reconstruction accuracy R^2.

V. Result Analysis and Discussion

To explore the mechanism of balance recovery after pushing with four-level forces, the kinematic characteristics obtained from the subjects are analyzed and discussed in this section. We also study on the synergy structure alternation regarding W depending on the different levels of push.

From the extraction of spatial synergies shown in Fig. 2, the ratios of reconstruction accuracy, R^2, and synergy level are varying for the four-level pushing forces. The high ratio of synergy W_1 illustrates common balance recovery spatial feature for all levels in Fig. 2 (*a*). For the pushing force level 1, its ratio of W_1 is 0.96, which is almost equal to the total ratio from W_1 to W_3 for the pushing force from level 2 to 4. The eight joint angles can be reconstructed by the three synergies with the high $R^2 = (0.965 \pm 0.005)$ shown in Fig. 2 (*b*), which simplifies the kinematic motion modes. This illustrates that the high synergy level of balance recovery movements for the four-level pushing forces. Even though the reconstruction accuracy by the recruitment of three synergies are almost the same for level $2-4$ pushing forces, the combinations of joint angles and the ratio of R^2 in Fig. 2 (*a*) are different respects to the space of synergies W_1, W_2 and W_3. The synergy level of balance in Fig. 2 (*c*) is computed by the spatial surface area under curves of the reconstruction accuracy R^2. Although the high reconstruction accuracy exists with the recruitment of W_1, W_2 and W_3 for all pushing forces in this study, the synergy level seems depending on pushing force level. The synergy level decreases as the pushing force increases. This is reasonable as the limitation of joint capability caused by external disturbance leads to the reduction of synergy level.

We can also notice that there is synergy structure alternation regarding W depending on the different levels of push. Ankle angle variation in the space of W_1 is the strongest for the pushing force level 1 as Ch_7 and Ch_8 show the strongest intensity. This indicates that the ankle strategy exists for the

pushing force level 1 for small disturbance. The relative joint angle phase between ankle and hip in the space of W_1 is in-phase. Additionaly, there is only 1 motion mode for this level.

Secondly, from level 2, we observe there are 2 motion modes combined. The strong coordination of hip joints can be observed through the space of synergy W_1 for the pushing forces from level 2 to 4 as Ch_3 and Ch_4 show the strongest intensity. This should indicate the employment of hip strategy from small level of push. The $1st$ mode W_1 reflects hip strategy. Then, we still observe the ankle strategy at the $2nd$ motion mode at W_2, as as Ch_7 and Ch_8 show the strongest intensity for W_2. Between level 2 and level 3, it demonstrates similar motion mode for W_1 and W_2. However, we can notice the anti-phase between ankle and hip joint angles in synergies W_2 is observed more clearly for level 3. The larger anti-phase of ankle and hip exists for balance recovery reflecting ankle-hip strategy. This opposite flexion of ankle joints relative to hip joints is a well-known balance strategy, for higher disturbing forces.

Then, for further strong push for level 4, arm usage can be noticed as as Ch_1 and Ch_2 show stronger intensity for W_2, and efforts of active arm swing increase as the pushing force increases, where arm strategy is applied for improving the ability of balance recovery. This result is in accordance with our previously obtained conclusion in reproduced balance recovery movements through nonlinear model predictive control (NMPC) [4], [5] that arm usage helps balance control. Second, the in-phase and anti-phase of the ankle and hip joint illustrates the switch of ankle strategy and hip-ankle strategy. This kind of joint recruitment improves the ability of balance recovery based on the previous conclusion stated in [2].

The evolution of the corresponding activation weights of the extracted spatial synergies of joint angles for the four-level pushing forces is illustrated in Fig. 3. C_1, C_2, C_3 represent time-related activation where the balance recovery process can be observed. As described in our human experiment protocols, for each level pushing force, each subject performs four trials. For each trial, the time of motion is limited to 3 seconds. There are twenty-four trials that can be observed for each level of pushing force. In C_1, the balance behavior can be well understood. Before the pick value of activation, subjects are pushed, and then they behave in the balance recovery process. Even though the pushing forces are divided into four levels, the balance recovery time is almost the same. This is because humans have the predictive ability and can adjust their standing postures very fast under the cooperation of CNS and body muscles.

VI. CONCLUSIONS

In this paper, various balance recovery motions for four different levels of pushing forces are classified as balance recovery approaches like arm strategy, ankle strategy and hip-ankle strategy based on the extracted spatial synergy. The common patterns and the high synergy level of balance recovery motions are confirmed as well, which indicates the strong coordination between joint angles based on the switch of balance recovery strategies. The proposed method in this paper implements a quantitative classification of balance control strategies through the extracted kinematic spatial synergy metric. Therefore, our method is different from the traditional analysis of joint angle trajectories for classifying balance strategies. The synergy level is computed to further study the performance of human joint capability for the different pushing forces. In future studies, we study the coordinated motion patterns for more subjects and with more different conditions to further understand the relationship between the extracted spatial synergies and balance postural control strategies.

REFERENCES

[1] DA. Winter, Human balance and posture control during standing and walking, Gait and Posture, vol. 3, no. 4, pp. 193–214, Dec. 1995.

[2] AD. Kuo, FE. Zajac, Human standing posture: multi-joint movement strategies based on biomechanical constraints, Progr. Brain Research, vol. 97, pp. 349-358, Jan, 1993.

[3] K. Shen, A. Chemori and M. Hayashibe, Human-Like Balance Recovery Based on Numerical Model Predictive Control Strategy, IEEE Access, vol. 8, pp. 92050-92060, 2020.

[4] K. Shen, A. Chemori and M. Hayashibe, Effectiveness Evaluation of Arm Usage for Human Quiet Standing Balance Recovery through Nonlinear Model Predictive Control, 2020 3rd International Conference on Control and Robots, Dec. 26-29, 2020.

[5] K. Shen, A. Chemori and M. Hayashibe, Reproducing Human Arm Strategy and Its Contribution to Balance Recovery Through Model Predictive Control, Frontiers in Neurorobotics, 15:679570, 2021. doi: 10.3389/fnbot.2021.679570.

[6] JH. Allum, F. Honegger and CR. Pfaltz, The role of stretch and vestibulo-spinal reflexes in the generation of human equilibrating reactions. Prog Brain Res., Vol.80, pp.399-409, 1989.

[7] N. Bernstein, The Co-ordination and Regulation of Movement, Oxford, 1967.

[8] W. Hsu, L. Chou and M. Woollacott, Age-related changes in joint coordination during balance recovery, Age, Vol. 35, pp. 1299-1309, 2013.

[9] WA. Lee, Neuromotor synergies as a basis for coordinated intentional action, Journal of Motor Behavior, vol. 16, pp. 135-170, 1984.

[10] A. d'Avella, M. C. Tresch, Muscle Synergies for Motor Control, Handbook of Neural Engineering, pp. 449-465, 2006.

[11] P. Haggard, K. Hutchinson and J. Stein, Patterns of coordinated multi-joint movement, Exp. Bra. Res., Vol. 107, pp.254-266.

[12] J. Chai, M. Hayashibe, Motor Synergy Development in High performing Deep Reinforcement Learning algorithms, IEEE Robotics and Automation Letters, Vol. 5, pp. 1271-1278, 2020.

[13] N. Yang, Q. An, H. Yamakawa, Y. Tamura, A. Yamashita and H. Asama (2017) Muscle synergy structure using different strategies in human standing-up motion, Advanced Robotics, Vol. 31:1-2, pp. 40-54, 2017.

[14] H. Yamasaki, S. Shimoda, Spatiotemporal modular organization of muscle torques for sit-to-stand movements, J. Biomechanics, Vol. 49, pp. 3268-3274, 2016.

[15] G.Hettich, L. Assländer, A. Gollhofer, T. Mergner, Human hip–ankle coordination emerging from multisensory feedback control, Human Movement Science, Vol. 37, pp. 123-146, 2014.

[16] AV. Alexandrov, AA. Frolov, J. Massion, Biomechanical analysis of movement strategies in human forward trunk bending. I. Modeling. Biol Cybern, Vol. 84, pp. 425–434, 2001.

[17] AMTI Force Plates website: https://www.amti.biz.

[18] A. Seth et. al., OpenSim: Simulating musculoskeletal dynamics and neuromuscular control to study human and animal movement. PLoS Comput Biol., Vol. 14(7):e1006223, 2018.

[19] SR. Hamner and SL. Delp, Muscle contributions to fore-aft and vertical body mass center accelerations over a range of running speeds, J. Biomech., vol. 46, pp. 780–787, 2013.

[20] OptiTrack website: http://www.optitrack.com.

[21] IT. Jolliffe and J. Cadima, Principal component analysis: a review and recent developments,Phil. Trans. R. Soc. A.37420150202, 2016.